# Nonsequential double ionization of molecular fragments

Chunlei Guo,* Ming Li, John P. Nibarger, and George N. Gibson
*Department of Physics, University of Connecticut, Storrs, Connecticut 06269*
(Received 18 October 1999; published 15 February 2000)

High-precision ion yields are taken with 30-fs ultrashort laser pulses in various species of doubly ionized diatomic molecules, $N_2$ and $O_2$, including metastable, charge symmetric, and asymmetric dissociating channels. The experimental results indicate that the detailed electronic structure is a critical factor influencing strong field nonsequential ionization. The study of ellipticity effects of nonseqential ionization is also extended, for the first time to our knowledge, to the molecular system.

PACS number(s): 33.80.Rv, 33.80.Wz, 42.50.Hz

## I. INTRODUCTION

With advances in high intensity ultrashort-pulse lasers, the phenomena that relate to multielectron effects have drawn more and more attention in strong field laser physics during the past decade. Among these phenomena, nonsequential (NS) double and multiple ionization of atoms and molecules is one of the most interesting and challenging problems. NS ionization normally involves an enhancement in the double or multiple ionization yields compared to calculations based on sequential processes. In the case of helium in a linearly polarized field, for example, an unambiguous enhancement of the double ionization rate was observed [1,2]. It has been argued that the enhancement must be due to a direct, nonsequential process instead of a resonance process [1,3]. Based on the intensive experimental studies on this problem, many properties of NS ionization have been established. First, the knee structures of the enhanced double and multiple ion yields could be fit with the tunneling rate of lower charge states, and this implies that NS ionization is related to the tunneling process [2,4]. Second, the NS ionization rate is substantially suppressed by using circularly polarized light, which shows that NS ionization has a strong ellipticity dependence [3]. Last, it is shown that the pulse duration has little influence on NS ionization, but NS behavior is wavelength dependent [5].

Two theoretical models have been proposed to explain the experimental observations. On the one hand, the so-called ''shake-off'' model suggests that as one electron is ionized, another electron could be ''shaken off'' into the continuum due to the rearrangement caused by the sudden removal of the first electron [1]. However, this ''shake-off'' model is still not fully tested due to the extreme demands of a realistic calculation. On the other hand, the ''rescattering'' model states that an electron can collide with its parent ion core one-half cycle after being ionized by a laser field, and this $e$-$2e$ rescattering could lead to an enhanced double ionization [6]. However, the rescattering model fails to predict the observed NS threshold and magnitude [2].

Even though many theoretical investigations have been performed in studying NS ionization, the studies are mainly limited to the helium atom due to the increasing difficulty of treating larger atoms [7–9]. The insufficient understanding of the mechanism of NS ionization is due not only to the theoretical difficulty in treating the problem exactly; but further experimental investigations are also necessary to direct the theoretical studies. Recently, we reported the experimental observation that diatomic molecule $N_2$ behaves like a structureless atom in both single and double ionization, while $O_2$ behaves anomalously, having both a low single and NS double ionization rate [10]. The observation strongly indicates that the detailed electronic structure plays a key role in influencing the NS double ionization since $N_2$ has a closed shell electronic structure, while the outermost orbital $(1\pi_g)^2$ of the ground state of $O_2$ is only half filled. Because of the extra degrees of freedom, molecules can provide important tests in the detailed electronic structure point of view due to a greater diversity of electronic states and energy levels associated with their metastable and dissociating ions. In this paper, by carefully separating the different fragmentation channels in the time-of-flight (TOF) spectrum and by eliminating the effects of enhanced ionization of molecules at critical internuclear separation by using 30-fs ultrashort laser pulses [11,12], we made high-precision ion yield measurements on three pathways of doubly ionized $N_2$ and $O_2$, including metastable (e.g., $N_2^{2+}$), charge symmetric dissociating (CSD, e.g., $N_2^{2+} \rightarrow N^+ + N^+$), and charge asymmetric dissociating fragments (CAD, e.g., $N_2^{2+} \rightarrow N^{2+} + N$). Through studying the electronic states of these channels, we found further evidence that NS double ionization is strongly influenced by the detailed electronic structures of different molecular species. Ellipticity effects on NS ionization are also investigated in these molecular fragments.

## II. EXPERIMENTAL SETUP

The laser used in the experiment is a Ti:sapphire system running at a 1 kHz repetition rate, producing over 400 $\mu$J/pulse in 30-fs pulses with a central wavelength of 800 nm [13]. The laser pulses are focused with an on-axis parabolic mirror in a high vacuum chamber (base pressure $<5\times10^{-10}$ torr). Ions are extracted by a 135 V/cm dc field through a 1 mm diameter pinhole, accelerated over a 1260 V/cm dc field region into the 0.46 m field-free region of a TOF mass spectrometer [14]. At the end of the TOF tube,

*Present address: Condensed Matter and Thermal Physics Group, Materials Science and Technology Division, Los Alamos National Laboratory, Los Alamos, NM 87545.

 

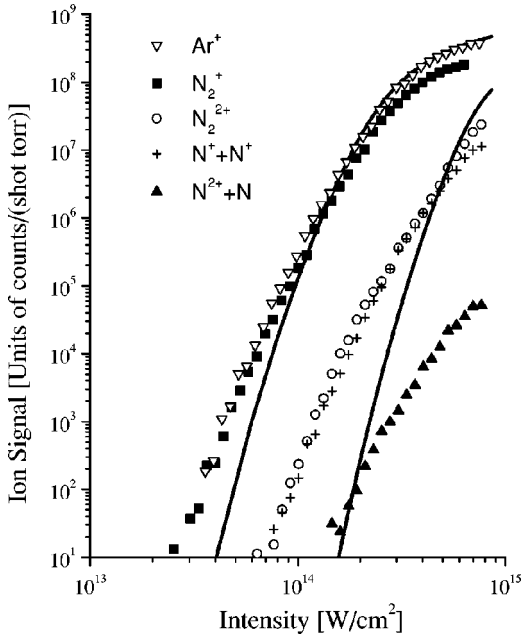


FIG. 1. Ion yields for $Ar^+$,$N_2^+$,$N_2^{2+}$, N(1,1), and N(2,0) with linearly polarized light. The full curves are the calculations based on the ADK model [16] to fit $Ar^+$,$N_2^+$,$N_2^{2+}$, and N(1,1). The ionization potentials used in the ADK model are the single and double ionization potentials for $N_2$, 15.58 eV and 27.12 eV [note that single ionization potentials for Ar and $N_2$ are very similar (Ar: 15.76 eV; $N_2$: 15.58 eV)]. The $N_2^+$ data are slightly reduced at the highest intensities due to detector saturation.

ions are detected with a microchannel plate as a function of flight time. This signal is further amplified, discriminated, and either integrated with a boxcar to produce ion yields or sent to a multihit time-to-digital converter (TDC) to generate the TOF spectrum. The TDC has a time resolution of 0.5 ns. The electron multiplier gain is approximately proportional to $Z/M^{1/2}$ [15], where $Z$ is the charge and $M$ is the mass of the ion. This factor needs to be taken into account since the studied ions have different charges and masses. An intensity window circuit is also used to take the TOF spectra, which restricts the data collection to an intensity range of 10%, hence minimizing the fluctuations of laser pulse energy. Absolute calibration of laser intensity is obtained by fitting the $Ar^+$ linear polarization ion yield to the ADK model [16], as shown in Fig. 1 and discussed in Ref. [10]. The absolute intensity agreed with the intensity calculated from the measured beam-spot size, pulse duration, and energy to within a factor of 2.

The dissociating ion pairs normally show symmetry in flight time around a zero-kinetic energy peak representing initial velocities either towards or away from the detector. A correlation technique is used to identify the dissociating channels. For example, in Fig. 2, the solid line is the spectrum of $N^+$ with data averaged from all the laser shots. We also averaged the data from only those laser shots containing a late-arriving $N^{2+}$ ion, shown with the dotted line. If $N^{2+}$ had no correlation with any peaks in this $N^+$ spectrum, the dotted line would represent an average of randomly selected data and would not affect the spectrum. However, if a correlation exists between the $N^{2+}$ and an $N^+$ peak, the dotted line will show a difference from the solid line reflecting this correlation. As shown in Fig. 2, the majority of the spectrum remains unchanged, but one peak clearly stands out and can be identified as $N_2^{3+} \rightarrow N^+ + N^{2+}$. With this correlation method, we can immediately identify most of the dissociating channels in TOF spectra, including CSD channels of doubly ionized $N_2$ and $O_2$. The metastable and CAD channels can be further deduced, as discussed in detail in Refs. [10,12,17].

High-precision intensity dependent ionization yield measurements are essential in order to study NS ionization. The ion yield data are normally obtained by integrating ion signals with a boxcar over a range of flight time, which corresponds to a certain ion species. When taking the ion yields for atoms, one can easily set the boxcar width wide enough to integrate over almost all the ion signal because the individual species are well separated from each other in the flight time. However, it is very difficult to isolate different molecular fragments for a certain charge state using a boxcar due to the small flight time separation between neighboring peaks. Ion yields of the molecular fragments cannot be valid unless both the boxcar width and delay time are set highly accurately. The fragment peaks can be well isolated when we set the width of the boxcar to be the full width at half maximum (FWHM) of the ion peaks, which is typically 10–20 ns, and can be set using a 1-GHz sampling rate digital oscilloscope. However, the delay time of the ion signal is an absolute time interval from a trigger point, which is not identical to the electronic pathway of the oscilloscope display. Therefore, it is extremely hard to set this delay time highly accurately

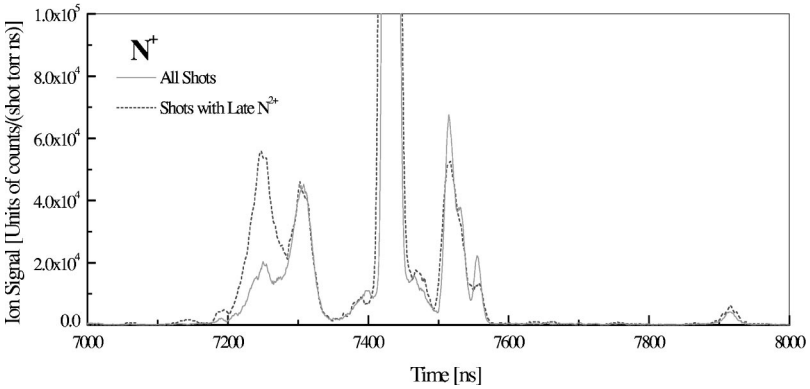


FIG. 2. Ion-ion correlation spectrum for $N^+$. The solid line is the spectrum of $N^+$ with data averaged from all the laser shots, while the dotted line shows data averaged from only the laser shots containing a late-arriving $N^{2+}$ ion.

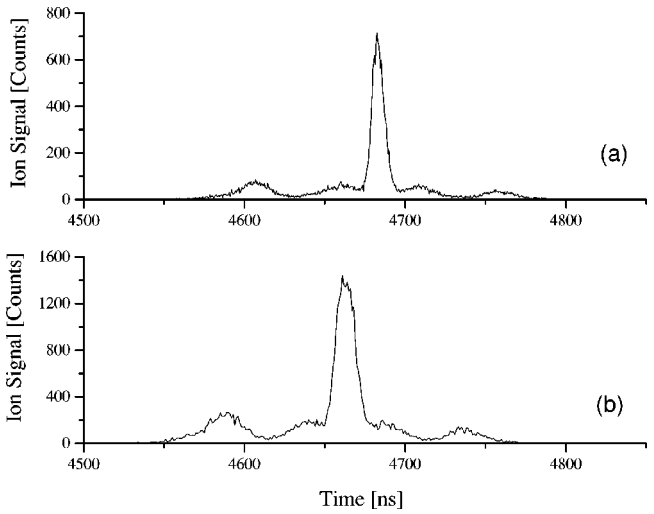


FIG. 3. (a) Normal time-of-flight (TOF) spectrum of $N^+$. (b) Time convolution of the TOF spectrum of $N^+$. The flight time of $N^+$ in this figure is different from Fig. 2 because different TOF spectrometer voltages are used.

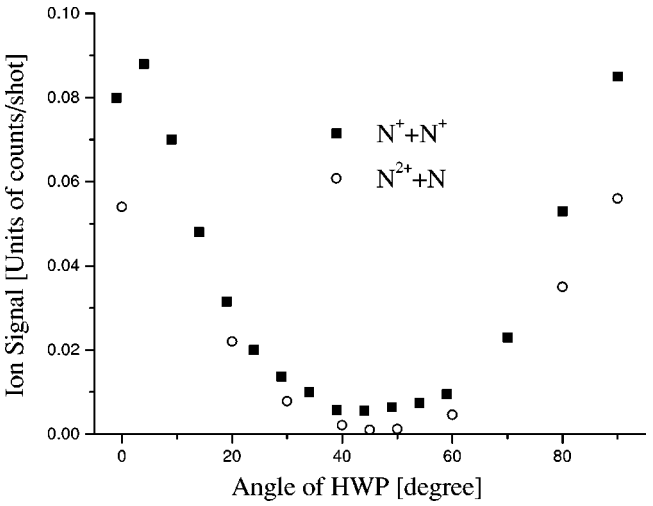


FIG. 4. Angular distribution for dissociation with respect to the incident *E* field of the laser. Channel N(1,1) is collected at intensity $3.7\times10^{14}$ W/cm$^2$, and N(2,0) is collected at intensity $8\times10^{14}$ W/cm$^2$.

without being able to make a direct measurement. In order to circumvent this obstacle, we developed a new technique to set an absolutely accurate delay time. The boxcar width is set to be equal to the FWHM of a particular peak, and the delay time is set by a digital delay generator (DDG) controlled by a computer. The delay time is stepped through a certain time range by the DDG, and a time convolution is made on a TOF spectrum by the scanning boxcar, shown in Fig. 3. We can then unambiguously determine the delay time of a particular peak from the time-convoluted spectrum. Once the delay time of the boxcar is set with this technique, the ion yield is taken with the boxcar width equal to the FWHM of the ion signal. The ion yields taken with this technique are almost free of neighboring fragment contamination.

In general, the dissociating channel $X_2^{(q1+q2)+}\rightarrow X^{q1+}+X^{q2+}$ is labeled as $X(q1,q2)$. Besides the thermal velocity distribution, fragments from molecules, unlike atoms, also acquire initial kinetic energy due to dissociation. TOF spectra are taken with different laser polarization angles by rotating a half-wave plate (HWP), and the integrated TOF signals of N(1,1), N(2,0), O(1,1), and O(2,0) are plotted in Figs. 4 and 5. We can see that the ion signal is the highest when the HWP is 0° or 90° with respect to the plane of the optical table, which corresponds to laser E field in the direction of the ion detector. The ion signal drops to a minimum when the HWP is at 45° corresponding to the laser E field perpendicular to the ion detector. These angular dependent ion signals clearly show that molecules preferentially dissociate along the laser *E* field. A three-dimensional angular distribution of the dissociating species is extrapolated from this experiment. A collection efficiency factor is obtained and taken into account in plotting all the dissociating ion yields.

### III. EXPERIMENTAL RESULTS AND DISCUSSION

The initial kinetic energy of dissociating ions can be determined from the TOF spectra. The results for both charge symmetric and asymmetric channels of doubly ionized $N_2$ and $O_2$ are

$$N_2^{2+}\rightarrow N^+ + N^+ + 7 \text{ eV},$$

$$N_2^{2+}\rightarrow N^{2+} + N + 1.5 \text{ eV},$$

$$O_2^{2+}\rightarrow O^+ + O^+ + 6.8 \text{ eV},$$

$$O_2^{2+}\rightarrow O^{2+} + O + 2.0 \text{ eV}.$$

The ionization threshold from the ground state of a neutral molecule to a dissociating fragment is determined by summing the following contributions: the energy necessary to dissociate the neutral molecule, the energy needed to ion-

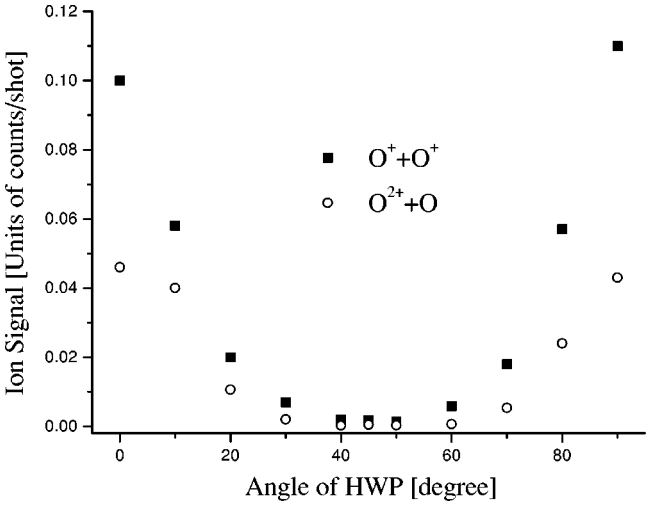


FIG. 5. Angular distribution for dissociation with respect to the incident *E* field of the laser. Channel O(1,1) is collected at intensity $3\times10^{14}$ W/cm$^2$, and N(2,0) is collected at intensity $7\times10^{14}$ W/cm$^2$.

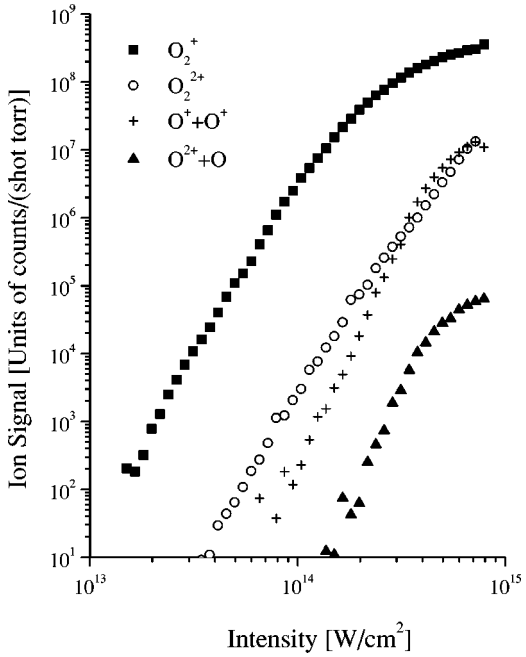


FIG. 6. Ion yields for $O_2^+$, $O_2^{2+}$, O(1,1), and O(2,0) with linearly polarized light.

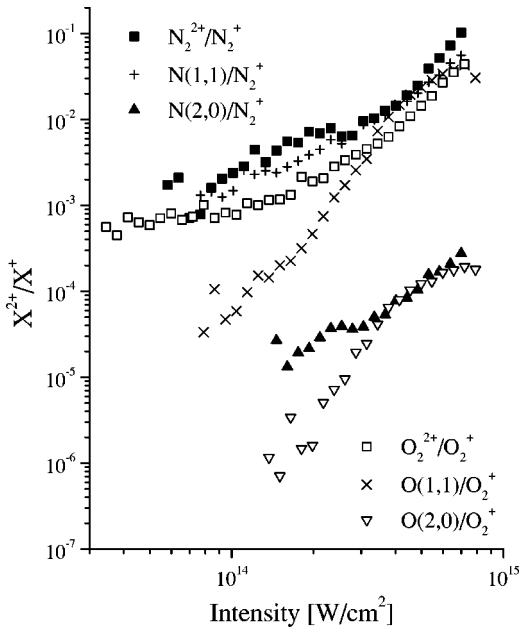


FIG. 7. Ratio curves of $X^{2+}/X^+$ for $N_2$ and $O_2$ with linearly polarized light.

ize each atom to its specific charge state, and the released kinetic energy. The resulting total energy is the energy level of a fragment channel if we assume that the dissociating fragments are in their ground state and, thus, only gives a lower bound. In fact, recent measurements indicate that dissociating channels can be in excited states [17]. The ionization potentials obtained by this method for N(1,1), N(2,0), O(1,1), and O(2,0) are 30 eV, 39.7 eV, 27.2 eV, and 44 eV, respectively, above the ground states of the corresponding singly ionized molecules. Ion yields of singly and doubly ionized $N_2$ and $O_2$, along with the dissociating channels, are plotted in Figs. 1 and 6 with linearly polarized light.

Nondissociating metastable channels of doubly ionized $N_2$ and $O_2$ have been discussed in detail elsewhere [10], and therefore we concentrate on the study of the dissociating fragments in this paper. The 7 eV kinetic energy release from the N(1,1) channel is consistent with previous results with 610 nm laser radiation and soft x-ray studies [18,19]. The dissociating ions N(1,1) are identified as being in the $^3P$ ground state, and they originate from the same molecular complex as metastable ground state $N_2^{2+}$. This is supported by the fact that the ion yields of $N_2^{2+}$ and N(1,1) almost overlap and have the same intensity dependence in agreement with Ref. [20]. In comparison, ion yields of $O_2^{2+}$ and O(1,1) have quite a different intensity dependence. From Fig. 6, we can see that the curves for $O_2^{2+}$ and O(1,1) actually cross. At the intensities below $2\times10^{14}$W/cm$^2$, the metastable state $O_2^{2+}$ dominates the process, but when the intensity goes above this value, the dissociating channel O(1,1) actually exceeds $O_2^{2+}$. This different and competing ionization behavior from two doubly ionized $O_2$ channels implies that $O_2^{2+}$ and O(1,1) originally come from different electronic states. The dissociating channel O(1,1) can be formed by removing one of the $1\pi_u$ inner binding orbital electrons resulting in a different electronic state from the metastable $O_2^{2+}$.

Generally, NS double ionization is characterized by a knee structure in double ionization yield compared to calculations based on sequential processes (e.g., see Fig. 1 for comparison between $N_2^{2+}$ data and the ADK model), but this cannot quantitatively measure the rate of NS double ionization. The intensity dependence of the ratio $X^{2+}/X^+$ has been used to indicate NS double ionization [2,10], where $X^+$ and $X^{2+}$ are the yields for single and double ionization of some atom or molecule, $X$ (e.g., $N_2^{2+}/N_2^+$ can show NS double ionization in a molecular system [10]). Nonsequential dynamics are most fundamentally related to this ratio: if $X^{2+}$ is produced in a sequential process, $X^+$ will be the intermediate species and the ratio $X^{2+}/X^+$ will reflect just the ionization rate from $X^+$ to $X^{2+}$ which will have a strong intensity dependence. However, if this ratio is only weakly dependent on intensity, it shows that the precursor to $X^{2+}$ is not $X^+$, and the ionization will involve the NS process. $N_2^{2+}$ and N(1,1) show almost the same intensity dependent ion yields, and the ratio curves for these two channels are also very close, as shown in Fig. 7. NS double ionization rates of both $N_2^{2+}$ and N(1,1) are higher than the other fragments, which is characterized by the weakly intensity-dependent part of the curves. $O_2^{2+}$ shows NS double ionization but at a distinctly reduced rate, more than five times lower than $N_2^{2+}$ and N(1,1). The ratio curve for O(1,1) drops monotonically with the decreasing intensity and does not show NS double ionization behavior within the experimental intensity range. It is clear now that N(1,1) and $N_2^{2+}$ have similar NS double ionization rates since they originate from the same molecular complex (discussed in the previous paragraph). However, NS double ionization exits in $O_2^{2+}$ but not in the dissociating channel

O(1,1), which must be due to their different electronic states. Furthermore, the different rates between molecules $N_2$ and $O_2$ can also be attributed to their different electronic configuration, as discussed in Ref. [10] between the metastable states of $N_2^{2+}$ and $O_2^{2+}$:$N_2$ has a closed-shell electronic structure, while the outermost orbital $(1\pi_g)^2$ of the ground state of $O_2$ is only half filled.

Charge asymmetric dissociation in molecules is itself an interesting question since the energy level of CAD lies much higher than the charge symmetric dissociation channels. Intuitively speaking, CAD can result from two or more electrons being driven from side to side in a molecule by a strong external field. If this was the case, these collective motions might have effects on NS ionization. Ion yields of CAD channels N(2,0) and O(2,0) are plotted in Figs. 1 and 6. Due to the higher ionization potential of CAD states, we can see that the ion yields of N(2,0) and O(2,0) are much smaller compared to CSD species N(1,1) and O(1,1), as shown in Figs. 1 and 6. The overall ratio curves of CAD are also lower than their CSD counterparts (Fig. 7). It should be noticed that the ratio curve of N(2,0) remains relatively constant at intensities lower than $4\times10^{14}$W/cm$^2$; however, the ratio of O(2,0) does not show any weak dependence on intensity. This indicates that there is an NS double ionization component in N(2,0) while NS double ionization does not appear to exist in O(2,0). Though we do not know the detailed electronic states of these two CAD channels, their different NS double ionization behaviors could also result from their different electronic structures, as argued above for metastable and CSD channels. Nevertheless, it is clear now that CAD can be formed through NS ionization like N(2,0), and can also be formed with a sequential process like O(2,0). There does not seem to be a direct relationship between NS ionization and the formation of CAD, and, in fact, a diversity of the pathway to form the CAD states shows that CAD is a natural result of strong field excitation and ionization with our 30-fs ultrashort laser pulses, as reported in Refs. [12,21].

It has been observed that NS ionization is substantially suppressed when atoms are exposed to circularly polarized light (CP) [3], and the ion yields of doubly ionized atoms with CP can be fit relatively well by the models based on the sequential process, even though their linear polarization counterparts have significant knee structures. This indicates that NS ionization has a strong ellipticity dependence. Since it is relatively difficult to fit any model to the molecular dissociating channels, intensity-dependent ratio curves, $X^{2+}/X^{+}$, of the charge symmetric and asymmetric dissociating channels for doubly ionized $N_2$ and $O_2$ with CP are again used to indicate NS double ionization. As shown in Fig. 8, all the ratio curves drop significantly with decreasing intensity indicating there is almost no NS double ionization component in these channels with CP. Therefore, for the first time to our knowledge, we extend the study of ellipticity effects to the molecular fragmentation channels, and provide further evidence of the generality of ellipticity effects on NS ionization.

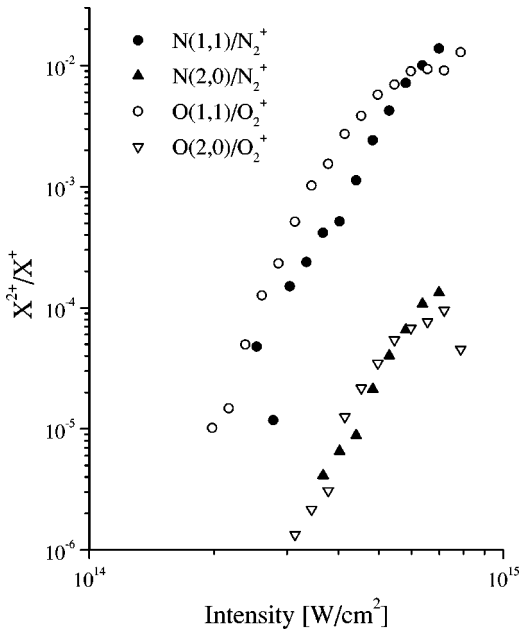


FIG. 8. Ratio curves of $X^{2+}/X^{+}$ for $N_2$ and $O_2$ with circularly polarized light.

## IV. CONCLUSION

In this paper, high-precision ion yields of metastable, CSD, and CAD channels in doubly ionized $N_2$ and $O_2$ have been measured and discussed. Species with different electronic structures behave quite differently in NS ionization, and these results show evidence that the strong field NS ionization is tied to the detailed electronic structure. We also show that the NS double ionization does not exist in the dissociating channels of $N_2$ and $O_2$ in a circularly polarized light. This indicates that ellipticity dependence persists in molecular fragments and appears to be a general property in NS ionization.

## ACKNOWLEDGMENTS

We would like to acknowledge support from the NSF under Grant No. PHY-9502935. G.N.G was also supported through funding by the Research Corporation.

[1] D.N. Fittinghoff, P.R. Bolton, B. Chang, and K.C. Kulander, Phys. Rev. Lett. **69**, 2642 (1992).

[2] B. Walker, B. Sheehy, L.F. DiMauro, P. Agostini, K.J. Schafer, and K.C. Kulander, Phys. Rev. Lett. **73**, 1227 (1994).

[3] B. Walker, E. Mevel, B. Yang, P. Breger, J.P. Chambaret, A. Antonetti, L.F. DiMauro, and P. Agostini, Phys. Rev. A **48**, R894 (1993).

[4] A. Talebpour, C-Y. Chien, Y. Liang, S. Larochelle, and S.L. Chin, J. Phys. B **30**, 1721 (1997).

[5] K. Kondo, A. Sagisaka, T. Tamida, Y. Nabekawa, and S. Wa-

tanabe, Phys. Rev. A **48**, R2531 (1993).
[6] P.B. Corkum, Phys. Rev. Lett. **71**, 1994 (1993).
[7] D.G. Lappas, A. Sanpera, J.B. Watson, K. Burnett, P.L. Knight, R. Grobe, and J.H. Eberly, J. Phys. B **29**, L619 (1996).
[8] J.B. Watson, A. Sanpera, D.G. Lappas, P.L. Knight, and K. Burnett, Phys. Rev. Lett. **78**, 1884 (1997).
[9] D.G. Lappas and R. van Leeuwen, J. Phys. B **31**, L249 (1998).
[10] C. Guo, M. Li, J.P. Nibarger, and G.N. Gibson, Phys. Rev. A **58**, R4271 (1998).
[11] T. Seideman, M. Yu. Ivanov, and P.B. Corkum, Phys. Rev. Lett. **75**, 2819 (1995).
[12] C. Guo, M. Li, and G.N. Gibson, Phys. Rev. Lett. **82**, 2492 (1999).
[13] G.N. Gibson, M. Li, C. Guo, and J. Neira, Phys. Rev. Lett. **79**, 2022 (1997); M. Li and G.N. Gibson, J. Opt. Soc. Am. B **15**, 2404 (1998).
[14] W.C. Wiley and I.H. McLaren, Rev. Sci. Instrum. **26**, 1150 (1955).
[15] C. Cornaggia, J. Lavancier, D. Normand, J. Morellec, P. Agostini, J.P. Chambaret, and A. Antone, Phys. Rev. A **44**, 4499 (1991).
[16] M.V. Ammosov, N.B. Delone, and V.P. Krainov, Z. Éksp. Teor. Fiz. **91**, 2008 (1986) [Sov. Phys. JETP **64**, 1191 (1986)].
[17] J.P. Nibarger, M. Li, S. Menon, and G.N. Gibson, Phys. Rev. Lett. **83**, 4975 (1999).
[18] C. Cornaggia, J. Lavancier, D. Normand, J. Morellec, and H.X. Liu, Phys. Rev. A **42**, 5464 (1990).
[19] W. Eberhardt, E.W. Plummer, I.-W. Lyo, R. Carr, and W.K. Ford, Phys. Rev. Lett. **58**, 207 (1987).
[20] C. Cornaggia and Ph Hering, J. Phys. B **31**, L503 (1998).
[21] G.N. Gibson, M. Li, C. Guo, and J.P. Nibarger, Phys. Rev. A **58**, 4723 (1998).